EUROFUSION WPJET1-CP(16) 15064

F Pizzo et al.

A 3D Electromagnetic Model of the Iron Core in JET

Preprint of Paper to be submitted for publication in Proceedings of 29th Symposium on Fusion Technology (SOFT 2016)

This work has been carried out within the framework of the EUROfusion Consortium and has received funding from the Euratom research and training programme 2014-2018 under grant agreement No 633053. The views and opinions expressed herein do not necessarily reflect those of the European Commission.

A 3D Electromagnetic Model of the Iron Core in JET

Andrea Gaetano Chiariello[1], Francesco Ledda[1], Raffaele Martone[1], Andrea Murari[2], Francesco Pizzo[1], Fernanda Rimini[3] and JET Contributors[a]

EUROfusion Consortium, JET, Culham Science Centre, Abingdon, OX14 3DB, UK

[1]Seconda Università degli studi di Napoli, Department of Industrial and Information Engineering, Aversa (CE), Italy
[2]EUROfusion Consortium, JET, Culham Science Centre, Abingdon, OX14 3DB, UK
[3]EURATOM-CCFE Fusion Association, Culham Science Centre, Abingdon, OX14 3DB, UK
[a]See the Appendix of F. Romanelli et al., Proceedings of the 25th IAEA Fusion Energy Conference 2014, Saint Petersburg, Russia

The Magnet and Power Supplies system in JET includes a ferromagnetic core able to increase the transformer effect by improving the magnetic coupling with the plasma. The iron configuration is based on an inner cylindrical core and eight returning limbs; the ferromagnetic circuit is designed in such a way that the inner column saturates during standard operations [1]. The modelling of the magnetic circuit is a critical issue because of its impact on several applications, including equilibrium and reconstruction analysis required for control applications. The most used model in present applications is based on Equivalent Currents (ECs) placed on the iron boundary together with additional specific constraints, in a 2D axisymmetric frame. The (circular) ECs are chosen, by using the available magnetic measurements, to best represent the magnetic polarization effect [1]. Due to the axisymmetric assumption such approach is not well suited to deal with significant 3D effects, e.g. arising in operations with Error Field Correction Coils (EFCC). In this paper a new methodology is proposed, based on a set of 3D-shaped ECs and able to better model the actual 3D magnetization. According to a well assessed approach [2], the 3D shape of ECs is represented by a set of elementary sources. The methodology has been successfully validated in a number of JET experiments where 3D effects are generated by EFCC currents. The new procedure has been designed to be easily coupled with equilibrium or reconstruction codes such as EFIT/V3FIT.

Keywords: JET, Iron core, Tokamak, Nuclear Fusion

1. Introduction

Ferromagnetic materials in fusion devices may have a strong impact on plasma boundary reconstruction analyses because of their effect on the nominal magnetic flux density map. In particular, iron core transformers were introduced in several tokamaks like JET [3] and GOLEM [4] to improve the magnetic coupling with the plasma.

In JET, most of the boundary reconstruction analyses are carried out by using 2D axisymmetric approximations of the plasma behavior, and, therefore, 2D models of the iron core. However, in some cases, e.g. pulses with Resonant Magnetic Perturbations (EFCC) for ELM mitigation studies [5], the availability of a model for the approximation of the 3D response of the iron core could be useful.

One of the main models, presently used at JET to take into account the iron effect, was proposed by [1] in 1992. The idea is based on the use of equivalent axisymmetric surface currents, placed along the iron-air interface (see Fig. 1), in order to approximate the iron behavior in a relatively far region of space. This model (or its variants) is usually adopted by 2D reconstruction codes like EFIT [6],[7].

In this paper, a 3D generalization (see Fig. 2) of [1] is proposed and, in addition, its implementation is discussed.

According to [1], the iron is modeled on the basis of its effect on the magnetic field, as revealed by the diagnostic system. Therefore, the problem can be reduced to the solution of a linear system with suitable accuracy. This can be very useful when speed is one of the main requirements as in control applications.

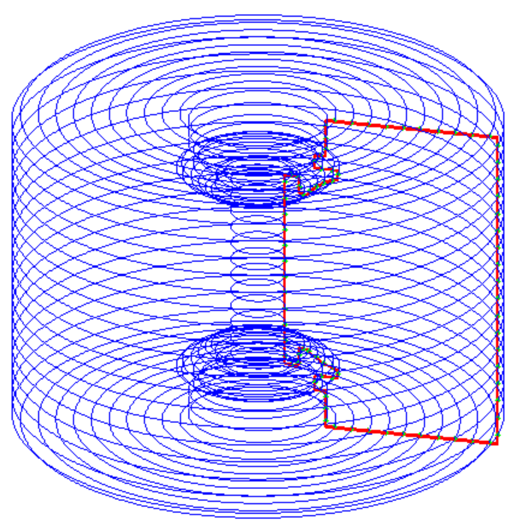

Fig. 1 – Axisymmetric equivalent currents (in blue) following the iron cross-section (in red).

The paper is organized as follows. In sect. 2 the mathematical formulation of the proposed model is shown whereas in sect. 3 numerical tools for the evaluation of the magnetic flux density generated by 3D configurations are suggested. In sect. 4 several results on 3D JET pulses are presented, in order to assess the model and the code. Finally, conclusions are drawn in sect. 5.

2. Mathematical Formulation

The magnetic characteristic of a material can be described by the classical equation:

$$\mathbf{B} = \mu_0 \mathbf{H} + \mu_0 \mathbf{M}(\mathbf{B}) \tag{1}$$

where $\mathbf{B}$ is the magnetic flux density, μ_0 is the magnetic permeability of the vacuum, $\mathbf{H}$ is the magnetic field and $\mathbf{M}$ the magnetization vector, vanishing in the air.

It is useful to recall that, at the iron-air interface, the tangential component of $\mathbf{B}$ is not continuous; this discontinuity, in the isotropic assumption, can be represented as a surface current, with a density k_m:

$$B_t^{iron} - B_t^{air} = \mu_0 k_m. \tag{2}$$

It should be noticed that the non-linear relation (1), between the magnetic flux density and the magnetization of the iron, can be expressed in terms of relative permeability; therefore, the boundary condition (2) can be rewritten as:

$$B_t^{iron} = \mu_0\, \mu_r(B^{iron}, \mathbf{r})\, H_t^{iron}. \tag{3}$$

where the dependence on the generic point $\mathbf{r}$ of the interface can be omitted in case of homogeneous assumption.

Furthermore, the tangential magnetic field H_t is continuous on the interface; therefore, it follows that:

$$B_t^{iron} = \mu_r\, B_t^{air} \tag{4}$$

where, from now on, the dependence of μ_r on B will be omitted for the sake of readability.

The approach used in this paper models the 3D effects of JET iron core, suitably discretized in a number of bricks, by means of surface currents flowing on their boundaries.

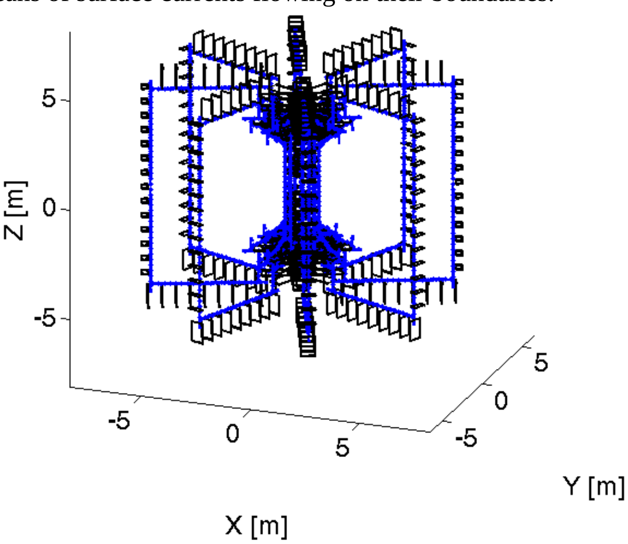

Fig. 2 – An example of 3D equivalent currents.

In the hypothesis that the current density k_m has the same direction for all the bricks (hypothesis that will be removed in the following) and by substituting (4) in (2), it is possible to obtain the non-linear equation relating the total magnetization current at the interface of the m-th brick with the magnetic flux density at the interface, as shown in [1].

It is interesting to note that, by using the implicit definition of relative permeability given by (3), an equivalent current has to be considered also in the saturated parts of the iron, because μ_r becomes:

$$\mu_r = 1 + \frac{B_{sat}}{\mu_0 H}. \tag{5}$$

Therefore, the equivalent current required to reproduce the effect of (3) is negligible only in the limit of $\mu_0 H \gg B_{sat}$.

Furthermore, for the simply connected unsaturated iron parts, the tangential component of the magnetic flux density at the boundary can be neglected:

$$B_t^{air} \cong 0 \qquad \text{when} \quad \mu_r \gg 1 \tag{6}$$

From the point of view of the plasma boundary reconstruction, the iron core generates a not negligible effect in the plasma region, which is relatively far from the iron. This effect can be estimated by considering a set of iron equivalent sources (e.g. the surface currents on the 3D iron interface).

The strength of the equivalent sources can be obtained by solving an inverse problem, starting from a set of magnetic measurements $\underline{m_d}$ coming from the diagnostic system (pick-up coils, flux loops, saddle coils etc.).

If the promptness is a strong requirement, it is possible to design an inverse problem by means of a linear system of equations and using the boundary condition (6) as virtual tangential probes placed on the interface.

In particular, the known part of the system becomes:

$$\underline{m} = [\underline{m_d} \quad \underline{m_v}]^T \tag{7}$$

where $\underline{m_v}$ is the array of virtual measurements (B_t=0).

On the other hand, the unknowns are represented by the components of the linear current density flowing on the boundary of all the bricks, collected in the array $\underline{k}$:

$$\underline{m} = \underline{\underline{G}}\, \underline{k} \tag{8}$$

where $\underline{\underline{G}}$ is a matrix relating the surface currents (causes) to the magnetic measurements (effects), which can be assumed to be known as will be shown in the next section.

3. Numerical implementation

In this section, a number of remarks for the implementation of the 3D iron core model will be given. First of all, it should be noticed that, due to the absence of magnetization in the air region, the surface current flowing on the brick boundary has the same amplitude of M_t on the iron.

$$M_t^{iron} - M_t^{air} = k_m \tag{9}$$

Therefore, from the numerical point of view, it is possible to take advantage of the analytical expressions of the magnetic flux density generated by a uniform magnetization in a brick [8],[9] as well as by surface currents, possibly discretized in a number of filamentary sticks [10].

In this paper the magnetization components, in a suitable coordinate system, of all the bricks have been considered as unknowns of the inverse problem, therefore:

$$\underline{m} = \underline{\underline{G}}\, \underline{M} \tag{10}$$

where $\underline{M}$ is an array collecting the magnetization components of all the N bricks (number of unknowns: 3xN).

Therefore, the response matrix $\underline{\underline{G}}$ can be simply evaluated by using the analytical expressions available in [8],[9],[10].

The linear system in (10) is ill-posed; furthermore, data in $\underline{m}$ can be strongly inhomogeneous because coming from different probes (pick-up coils measurements, flux measurements, boundary conditions etc.) which have different measurements uncertainties.

In order to cope with these problems, several measures can be taken, including:

a) each set of equations can be normalized to the total number of measurements of the same class (e.g. pick-up coils);
b) each set of probes can be weighted by a factor inversely proportional to the estimated error of that class of probes;
c) finally, a regularization of the linear system (10) can be carried out.

In this paper, the Tikhonov regularization has been adopted:

$$\underline{\underline{W}}\,\underline{m} = \underline{\underline{W}}\,\underline{\underline{G}}\,\underline{M}$$
$$\underline{M} \cong \left[\left(\underline{\underline{W}}\,\underline{\underline{G}}\right)^{T} \underline{\underline{W}}\,\underline{\underline{G}} + \underline{\underline{\Gamma}}^{T}\underline{\underline{\Gamma}}\right]^{-1} \left(\underline{\underline{W}}\,\underline{\underline{G}}\right)^{T} \underline{m} \qquad (11)$$
$$\underline{\underline{\Gamma}} = \alpha \underline{\underline{I}}$$

where $\underline{\underline{W}}$ is the diagonal matrix of weights which implements the point a) and b) of the previous list, $\underline{\underline{\Gamma}}$ and $\underline{\underline{I}}$ are the Tikhonov and identity matrix respectively and, finally, α is the Tikhonov parameter.

It should be noticed that Tikhonov regularization minimizes both the residual and the energy of the estimated solution on the basis of the α parameter:

$$\min_{\underline{M}} \left\|\underline{\underline{W}}\,\underline{\underline{G}}\,\underline{M} - \underline{\underline{W}}\,\underline{m}\right\|^{2} + \alpha^{2}\left\|\underline{M}\right\|^{2} \qquad (12)$$

In this paper, the α parameter has been chosen as a trade-off between the desire of small residuals and the need of a smooth solution; this can be achieved by using a L-curve criterion, as shown in [11][12].

The weights in $\underline{\underline{W}}$ can be also changed iteratively by means of the information coming from the results and on the basis of the ability of the solution to match data not used in the inverse problem. This point will be discussed further in the next section.

4. Example of Application

In order to assess the model, the procedure has been tested on JET Error Field Correction Coils shots and in particular on dry runs (without plasma), to isolate the iron effect.

The iron core geometry has been discretized by N_B=160 bricks (therefore, N_Bx3 unknowns), with a finer discretization for the polar shoes (see Fig. 3), while the boundary condition B_T=0 has been checked on N_V=864 points.

The diagnostic system used for the following example includes:

1. 18x4 pick-up coils;
2. 14x4 saddle loops;
3. 4 flux loops.

All the signal are taken from the JET Pulse File (JFP) server and have been corrected with standard TF-compensation procedures.

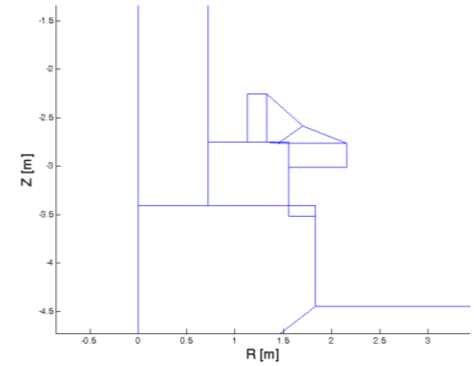

Fig. 3 – Polar shoes bricks' discretization.

In order to explore the capability of the procedure in reproducing an acceptable magnetic field in regions where no probes are present, a subset of 4 pick-up coils has been removed by the diagnostic data used to solve (11) and, instead, they have been used as a test set.

A relative error index has been computed for each class of probes used to solve (11), and for the subset of pick-up used to measure the generalization ability of the solution found.

$$Err = \frac{\left\|\underline{m} - \underline{\tilde{m}}\right\|_2}{\left\|\underline{m}\right\|_2} \qquad (13)$$

where $\underline{\tilde{m}}$ is the array of reconstructed measurements obtained by means of the solution of (11).

The first shot analyzed is the #86570 at T=73s, which is an EFCC shot with an n=2 mode along the toroidal direction (see Fig. 4).

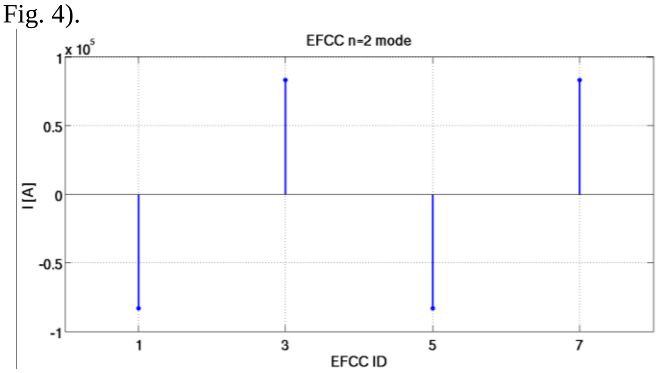

Fig. 4 – EFCC current.

The weight used for the virtual probes has been chosen as a factor of the one used for the real pick-ups, in the logarithmic range [10^{-10}, 10^{1}], as the one that minimize the error (13) on the test set.

In Tab. I, the results in terms of reconstruction errors are reported, together with a comparison with an implementation of the classical 2D model of the iron core [1].

Table I: reconstruction errors #86570@T=73s

Diagnostic set	2D reconstruction *Err %*	3D reconstruction *Err %*
Pickup coils	45.8 %	1.50 %
Flux loops	1.65 %	1.85 %
Saddle coils	37.4 %	4.09 %
Test set	46.2 %	5.96 %

The inability of 2D models in reconstructing the iron effect in an EFCC shot is better understood looking at its effect on the four replica of one single probe along the toroidal direction (see Fig. 5). The n=2 mode imposed by the EFCC magnetize the iron in different ways, depending on the position of each arm. Therefore, an axisymmetric model of the iron cannot reproduce such effects depending φ. Of course, an average along the toroidal direction can be considered but, in this case, due to the periodicity the 3D effects are lost.

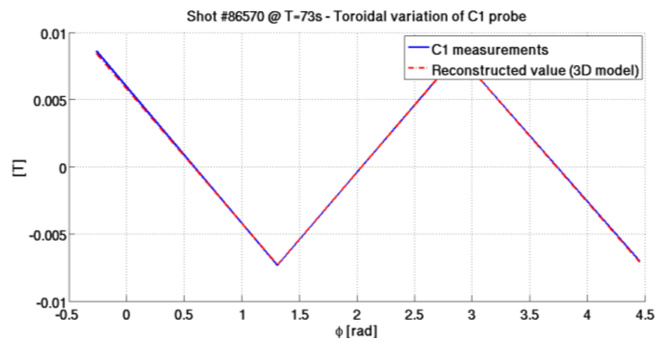

Fig. 5 – Iron effect reconstructed along φ direction.

On the other hand, if the iron excitation is given only by the axisymmetric active coil (such as poloidal field coils or the central solenoid), a 2D model produces of course a good approximation of the actually 3D iron core. Indeed, considering the same dry run (#86570) at T=52s, when the EFCC are not used but only the poloidal coils are active, the iron response is approximated much better, as reported in Tab. II and in Figs. 6-8.

Table II: reconstruction errors #86570@T=52s

Diagnostic set	2D reconstruction *Err %*	3D reconstruction *Err %*
Pickup coils	2.59 %	0.69 %
Flux loops	2.04 %	1.34 %
Saddle coils	3.05 %	2.29 %
Test set	2.60 %	1.40 %

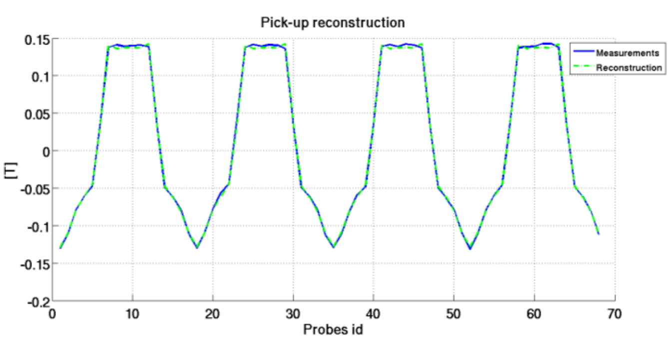

Fig. 6 – Pick-up measurements reconstruction.

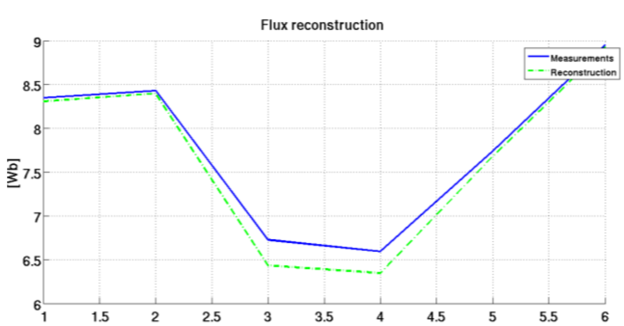

Fig. 7 – Flux measurements reconstruction.

Fig. 8 – Saddle coil measurements reconstruction.

5. Conclusions

A 3D model for the JET iron core has been proposed and tested. The model is able to reproduce the effects of the iron magnetization in a relatively far region (plasma region) and it is particularly effective when there are strong 3D excitations.

It has also been shown that when the excitation is axisymmetric, although the iron core remains 3D, its effects in the plasma region are well reproduced by the 2D model, within an error bar comparable with probes uncertainties.

Furthermore, the 3D iron equivalent sources reconstruction requires only the solution of a linear system. This feature makes the model particular effective in coupling with other codes, such as plasma boundary reconstruction procedures, which will be presented in subsequent papers.

References

[1] O'Brien D. P., et al. "Equilibrium analysis of iron core tokamaks using a full domain method." Nuclear fusion 32.8 (1992):1351.

[2] Chiariello A. G., et al. "Effectiveness in 3-D Magnetic Field Evaluation of Complex Magnets." IEEE Trans.Magn., vol.51.3, 2015.

[3] Rebut, P. H., R. J. Bickerton, and Brian Edgar Keen. "The Joint European Torus: installation, first results and prospects." Nuclear fusion 25.9 (1985): 1011.

[4] Markovič, Tomáš, et al. "Evaluation of applicability of 2D iron core model for two-limb configuration of GOLEM tokamak." Fusion Engineering and Design 88.6 (2013): 835-838.

[5] Liang, Y., et al. "Active control of type-I edge-localized modes with n= 1 perturbation fields in the JET tokamak." Physical review letters 98.26 (2007): 265004.

[6] L. Appel, et al. "A Unified Approach to Equilibrium Reconstruction", Proc. of the 33rd EPS Conference, no. 06, Rome, 2006

[7] Lao, L. L., et al. "Reconstruction of current profile parameters and plasma shapes in tokamaks." Nuclear fusion 25.11 (1985): 1611.

[8] Fabbri, Massimo. "Magnetic flux density and vector potential of uniform polyhedral sources." IEEE Transactions on Magnetics 44.1 (2008): 32-36.

[9] Chiariello, Andrea G., et al. "Effective magnetic field computation in Tokamaks in presence of magnetic materials." Fusion Engineering and Design 96 (2015): 641-644.

[10] Chiariello, Andrea Gaetano, Alessandro Formisano, and Raffaele Martone. "Fast magnetic field computation in fusion technology using GPU technology." Fusion Engineering and Design 88.9 (2013): 1635-1639.

[11] Hansen, Per Christian. "Analysis of discrete ill-posed problems by means of the L-curve." SIAM review 34.4 (1992): 561-580.

[12] Hansen, Per Christian, and Dianne Prost O'Leary. "The use of the L-curve in the regularization of discrete ill-posed problems." SIAM Journal on Scientific Computing 14.6 (1993): 1487-1503.